Hit Me With Your Best Shot; Using Elliptical Craters to Examine the Bombardment Source for Craters on Saturn's Moon Mimas. Sierra N. Ferguson[1], Alyssa R. Rhoden[1], Michelle R. Kirchoff[1] [1]Southwest Research Institute, Department of Space Studies, 1050 E Walnut St, Suite 300, Boulder Colorado, 80302, (sierra.ferguson@swri.org)

Introduction: Mimas is the inner most major moon of Saturn, and its history is inexorably tied to Saturn's rings [e.g., 1]. Mimas is thought to be a geologically dead world due to the relative lack of tectonics in comparison with the other ocean-bearing icy satellites [2] and the predominance of unrelaxed impact craters on the surface [3,4]. This apparent absence of geologic activity suggests that Mimas has never hosted an ocean underneath its ice shell because an ocean should give rise to high tidal stress and fractures, similar to those observed on other ocean-bearing, icy moons in eccentric orbits [e.g., 2]. However, examinations of Mimas' libration, as observed by the *Cassini* spacecraft [5], imply that either Mimas has an irregular core or that Mimas currently has an ocean underneath a 24-31 km thick ice shell [5]. The phase of the libration is more consistent with an ocean [6,7]. Furthermore, recent analysis of the present-day tidal heating of Mimas [8] suggests that an ocean could currently exist underneath the ice shell. A present-day ocean within Mimas is not an obvious outcome of any current formation models [e.g., 9].

Determining the age of Mimas and how it formed has broader implications for the formation and evolution of all the mid-sized Saturnian satellites. Some satellite formation models have Mimas form out of Saturn's rings [10,11], while the other mid-sized moons are formed from the Saturn sub-nebula [12,13], thus placing Mimas' formation age commensurate with the age of the rings. Other dynamical modeling has suggested that Mimas could be as young as 100 Myr [14]. Additional thermal-orbital evolution modeling of the mid-sized satellites [9] has suggested that the oldest Mimas can be and still match the current orbital configuration of the system is 1 Byr old (relative to the age of the rings).

Previous crater counts conducted on Mimas' surface reported a relative model surface age of ~4 Byr [15]. This age estimate relied on approximations of impactor size-frequency distributions [e.g., 16] that have been shown to significantly differ from the crater populations on several Saturnian moons [17]. If a planetocentric population, unique to Saturn, has contributed to the crater populations on the moons, surface ages derived this way would be inaccurate.

Recent work on elliptical craters on Tethys and Dione [18,19] have provided a novel approach to characterizing the planetocentric component of the crater populations. Although more modeling work remains to fully interpret these signatures, further mapping on additional satellites will help additionally constrain the modeling work. Better estimates of the age of Herschel basin can also help constrain the longevity of the present-day ice shell thickness, which is only a factor of 2-3 thicker than the depth of Herschel [8, 20].

Elliptical craters provide a way to examine the impact angles and directions of the initial impactors that generated the craters [21-23]. The direction of that major axis generally follows the direction of motion the impactor took as it collided with the surface [21-24].

We've previously surveyed elliptical crater populations on two of Saturn's other moons, Tethys and Dione [18,19]. Our analysis suggested that elliptical craters in the equatorial latitudes between 30° N and 30° S on both moons are preferentially oriented in the East/West direction [18,19]. We interpreted this concentration as the result of gradual flattening of a debris disk that both moons experienced, although it is unclear whether each moon had a separate debris disk or were subjected to the same disk. Extending this survey to Mimas allows us to gauge the extent of this potential debris disk. In addition to the elliptical crater distributions, we are computing a new age for the Herschel impact basin adjusted using our elliptical crater results. Previous work by MRK using an unmodified chronology from [16] indicated an age anywhere from 0.1-3 Ga [e.g., 25]; implying new analysis is needed.

Methods: We've mapped and analyzed the elliptical crater population across the surface of Mimas spanning all longitudes and ranging in latitude from 60° N to 60° S using the current Mimas basemap [26]. The basemap was used for the initial mapping and identification of craters, and then higher-resolution individual *Cassini* ISS images were used to check the identification and crater shapes. Mapping was conducted in a simple cylindrical projection for the equatorial longitudes and was switched to a sinusoidal projection for 30-60° N/S. Additional image coverage of Mimas' North Pole has allowed us to extend the mapping in the northern latitudes. For this portion of the map, the images and basemap were re-projected into a north polar stereographic projection for mapping purposes.

Determination of elliptical crater status followed the protocol laid out in [18,19]. Crater counting for the purpose of age dating Herschel included mapping craters in and around the basin (out to 1 crater radii),

where the exterior basin counts focused on the likely ejecta blanket.

Results: On Mimas, we have tentatively classified 128 craters with ellipticities greater than 1.2 and 229 craters with ellipticities greater than 1.1. Figure 1A shows a rose diagram of the measured crater orientations for all craters with ellipticities of 1.2 and higher. What appears most striking is the apparent strong signal of N/S oriented craters. Out of the ≥1.2 ellipticity group, 37% of the craters are located above 45° N/S, thus dominating the signal on the rose diagram. Additionally, 65% of craters in the ≥1.1 ellipticity group are located above 45°N/S and once again dominate the signal in the rose diagrams (not shown). However, if craters above 45°N/S in both eccentricity groups are excluded from the rose diagrams, the plots show that the remaining elliptical craters are oriented in all directions (Fig. 1B). Crater counts for the purposes of age dating Herschel are still on-going and we will present those results and our derived model age.

Discussion: The stark change in crater orientation trends from the East/West signal on Tethys and Dione to the North/South signal we're currently observing on Mimas is quite surprising. We are actively investigating whether lighting conditions near the poles could play a role in the lack of observed East/West craters in the polar regions. Limb images from Mimas allowed for examination of the polar terrains above 60°N, but those images are often captured at more extreme lighting angles. If not due to image conditions, the outstanding question about the origin of these elliptical craters remains, especially with how it fits into the proposed origin scenarios in [18,19].

The more isotropic spread in the mid-latitudes, however, could be compatible with our idea that these elliptical craters could have recorded the evolution of a debris disk in the system. Or perhaps that the elliptical craters on Mimas record a different disruption event more closely tied to the evolution of the rings. We do stress that these results are preliminary and are still undergoing verification of the crater azimuths and analyzing the lighting angles of the north polar imagery. The story of the cratering history on Mimas is far from straightforward, but the craters point towards the already complex and fascinating history of this small moon.

Acknowledgments: We'd like to thank Dr. Emily Martin for help in obtaining the Mimas basemap and NASA's CDAP Program for supporting this work (Grant 80NSSC21K0535 awarded to A.R Rhoden.) This work also made use of the USGS ISIS3 software and PILOT web tool.

References:[1] Neveu, M., Rhoden, A.R., (2017), *Icarus*, 296, 183-196. [2] Rhoden, A.R., et al., (2017), *JGR-Planets*, 122, 2, 400-410. [3] Schenk, P. M., (1989), *JGR*, 94, 3813-3832. [4] White, O. L., et al. (2017), *Icarus*, 288, 37-52. [5] Tajeddine, R., et al. (2014), *Science*, 346, 6207, 322-324. [6] Caudal, G. (2017), *Icarus*, 286, 280-288. [7] Noyelles, B. (2019), *MNRAS*, 486 (2), 2947-2963. [8] Rhoden, A. R., & Walker, M. E., (2022), *Icarus*, 376. [9] Neveu, M., Rhoden, A.R., (2019), *Nature Astronomy*, 3, 543-552. [10] Salmon, J. & Canup, R., (2017), *AJ*, 836 (1), 109. [11] Charnoz S., et al., (2011), Icarus, 216 (2), 535-550. [12] Mosqueira, I., & Estrada, P. R. (2003*), Icarus*, 163, 198-231. [13] Mosqueira, I., & Estrada, P. R. (2003), *Icarus*, 163, 232-255. [14] Ćuk, M., et al., (2016), *AJ*, 820, 2, 97. [15] Kirchoff, M.R., & Schenk, P.M., (2010), *Icarus*, 206, 485-497. [16] Zahnle, K., et al., (2003), *Icarus*, 163, 263-289. [17] Ferguson, S. N., et al., (2020), *JGR-Planets*, 125 (9), 1-21. [18] Ferguson, S.N., et al., (2021), *52nd AAS Division on Dynamical Astronomy meeting*, id. 106.02., BAAS, 53. [19] Ferguson, S.N., et al., (2022), *EPSL*, in rev. [20] Moore, J. M., et al., (2004), *Icarus*, 171, 421-443. [21] Gault, D. E., & Wedekind J. A., (1978), *9th LPSC*, 3843-3875. [22] Bottke, W.F., et al., (2000), *Icarus*, 145, 108-121. [23] Elbeshausen D., et al., (2013), *JGR-Planets*, 118, 2295-2309. [24] Holo, S., et al., (2018), *EPSL*, 496, 206-214. [25] Kirchoff, M. R., and P. M. Schenk. *Early Solar Sys. Imp. Bomb., Abst. #3023*, 2008. [26] Roatsch, T., et al., (2018), *Planetary and Space Science*, 164, 13-18.

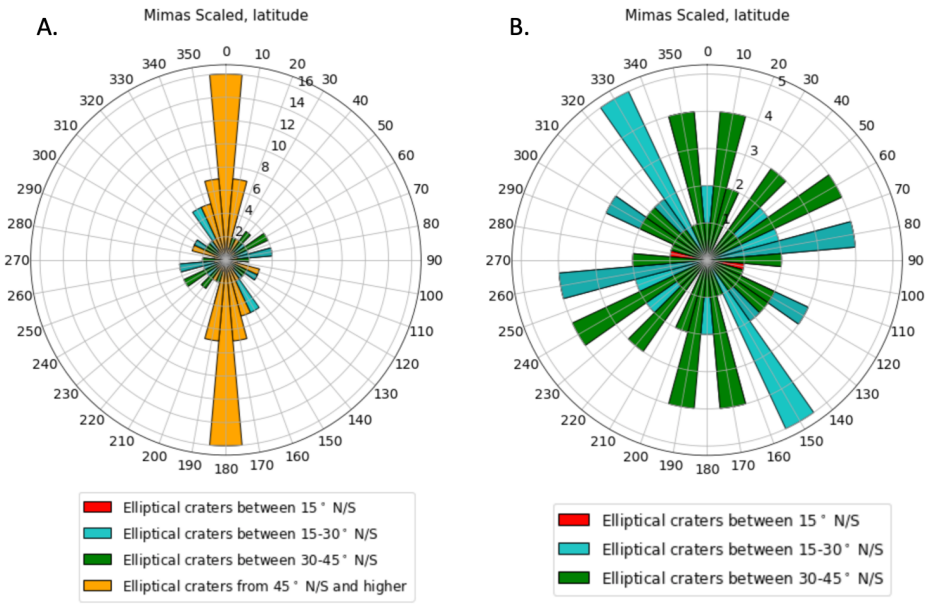

Figure 1A. Rose diagram of all mapped elliptical craters with ellipticities greater than 1.2. In this view, the N/S signal dominates the orientation distribution. **Figure 1B**. The same rose histograms for craters only between 45° S and 45°N. In this range, the elliptical craters are oriented in a more dispersed pattern.